EVLA Memo # 120
Some Thoughts on System Temperature Measurements for the EVLA

Rick Perley and Ken Sowinski

January 14, 2008

Abstract

We present an analysis of the required sensitivities of system temperature monitoring for the EVLA. Measurements taken from the VLA's system show excellent agreement with the theory. The WIDAR correlator presents both special challenges and great flexibility for measurement of system temperature. Some issues relevant to the WIDAR era are discussed.

1 Introduction

Both the current VLA and the new WIDAR correlators provide an estimate of the correlation coefficient for all pairs of input antenna signals. Conversion of the correlation coefficient to visibility amplitude requires adjustment by the antennas' system temperatures and efficiencies:

$$V_{ij} = \frac{2kC_{ij}}{A_p}\sqrt{\frac{T_i}{\epsilon_i}\frac{T_j}{\epsilon_j}} \tag{1}$$

where C_{ij} is the correlation coefficient measured between antennas 'i' and 'j' (following any necessary corrections for quantization and internal scaling), A_p is the physical aperture of the component antenna, ϵ is the aperture efficiency and T is the total system temperature.

Both the efficiency and system temperature of an antenna are functions of frequency, time and position. The efficiency is normally a known function of frequency and elevation only[1] so adjustment of the correlation coefficient for its effects is straightforward. The system temperature is a much more volatile quantity, as it depends on many factors with relatively short time-scales, including elevation, atmospheric conditions, source strength, and galactic coordinates, in addition to any changes in electronics. These dependencies require a real-time measurement system.

The system temperature is monitored by injecting a square-wave modulated known power into the front-end, and synchronously detecting the resulting increment in power at the correlator. The added power is switched at a frequency considerably higher than that of any expected change in system characteristics – typically a few Hz – and at a level large enough to allow an accurate measurement, but not so large as to seriously degrade sensitivity – typically about 5% of the system temperature. For a simple linear system with 'cal-off' state system temperature T_{sys}, and a 'cal-on' state system temperature $T_{sys} + T_{cal}$, the powers delivered to a power meter in the 'off' and 'on' states are $P_{off} = kT_{sys}GB$, and $P_{on} = k(T_{sys} + T_{cal})GB$, where B is the bandwidth and G is the system gain. With measurements of both P_{off} and P_{on}, the system temperature is

$$T_{sys} = T_{cal}\frac{P_{off}}{P_{on} - P_{off}}. \tag{2}$$

[1] This is true providing that antenna pointing is accurate, and that there are no reductions in source flux delivered to the receivers due to absorption by clouds.

2 Balancing Calibration Accuracy against Sensitivity Loss

The EVLA project book requires that changes in the total system power be monitored with an accuracy of $\leq$0.5% over changes on input system power of up to 15 dB over cold sky values. The intention of this requirement is to permit transfer of the flux density scale from a calibrator source of known flux density to a target source with an accuracy of better than 0.5%. This means that for a pair of visibility measurements on two sources, say 'A', and 'B', with antennas '1' and '2', the error in the ratio of their corrected visibilities be less than 0.5%. Presuming the efficiencies of the two antennas on the two sources are known and adjusted for, the derived visibility ratio R is given by

$$R = \frac{V_{A12}}{V_{B12}} = \frac{C_{A12}}{C_{B12}}\sqrt{\frac{T_{A1}T_{A2}}{T_{B1}T_{B2}}}. \tag{3}$$

Assuming that the errors in the determinations of the system temperature on the two sources for the two antennas are independent, then the fractional error in the measurement of the visibility ratio R is

$$\frac{\sigma_R}{R} = \frac{1}{2}\sqrt{\frac{\sigma^2_{TA1}}{T^2_{A1}} + \frac{\sigma^2_{TA2}}{T^2_{A2}} + \frac{\sigma^2_{TB1}}{T^2_{B1}} + \frac{\sigma^2_{TB2}}{T^2_{B2}}}. \tag{4}$$

This expression can be reasonably simplified by assuming that the fractional accuracy in the system temperature determination for both antennas on both sources is the same, in which case, we arrive at the simple answer

$$\frac{\sigma_R}{R} = \frac{\sigma_T}{T}. \tag{5}$$

Hence, for an accuracy of 0.5% in the transfer of the flux density scale, the fractional accuracy of the determination of system temperature for each antenna must be the same – 0.5%.

The system temperature is determined from Eq. 2, involving a ratio of two measured powers. Assuming the uncertainties in the determination of the two are uncorrelated, the fractional uncertainty in the cold-sky system temperature is

$$\frac{\sigma_T}{T_{sys}} = \frac{P_{on}}{P_{on} - P_{off}}\sqrt{\left(\frac{\sigma_{on}}{P_{on}}\right)^2 + \left(\frac{\sigma_{off}}{P_{off}}\right)^2}. \tag{6}$$

The uncertainty in the power measurement of duration τ seconds and bandwidth B Hz, is given by the radiometer equation

$$\frac{\sigma_P}{P} = \frac{1}{\sqrt{B\tau}}. \tag{7}$$

If the 'on' state occupies a fraction f of the time, so the 'off' state occupies a fraction $1 - f$, then the uncertainty in the measurement of T_{sys} can be written

$$\frac{\sigma_T}{T_{sys}} = \frac{T_{sys} + T_{cal}}{T_{cal}}\frac{1}{\sqrt{B\tau}}\frac{1}{\sqrt{f(1-f)}}. \tag{8}$$

This function is minimized when $f = 0.5$, giving

$$\frac{\sigma_T}{T_{sys}} = \frac{T_{sys} + T_{cal}}{T_{cal}}\frac{2}{\sqrt{B\tau}}. \tag{9}$$

It is useful to define a ratio $Q = T_{cal}/T_{sys}$, which measures the fractional rise in system temperature caused by the injected noise. In terms of this, the accuracy of the system temperature measurement is

$$\frac{\sigma_T}{T_{sys}} = \frac{2(1+Q)}{Q\sqrt{B\tau}} \sim \frac{2}{Q\sqrt{B\tau}}. \tag{10}$$

Providing $Q \ll 1$, a larger calibration signal results in a more accurate measure of the system temperature. However, the increment in noise power due to the calibration signal also degrades the system sensitivity. Denote by D the ratio of the interferometer sensitivity with the added calibration to that without. Then, (presuming a 50% duty cycle in the calibration),

$$D = \frac{T_{sys} + T_{cal}/2}{T_{sys}} = 1 + \frac{Q}{2} \tag{11}$$

This relation allows us to express the calibration accuracy result in terms of the loss in system sensitivity:

$$\frac{\sigma_T}{T} = \frac{2D-1}{D-1}\frac{1}{\sqrt{B\tau}} \sim \frac{1}{X\sqrt{B\tau}} \tag{12}$$

where $X = D - 1 = Q/2 = T_{cal}/2T_{sys}$, and the approximation assumes $X \ll 1$. The quantity X is the incremental loss in interferometer sensitivity caused by the calibration noise source. This equation quantifies the obvious statement that increasing calibration accuracy requires an increasing loss in sensitivity.

The fractional error in the determination of the visibility is inversely proportional to the degradation in the sensitivity caused by the calibration. A simple example taken from the VLA should be helpful in setting the scales: With a bandwidth of 50 MHz, and a time averaging of 1 second, obtaining an accuracy of 0.5% in the determination of the change in fractional system temperature will require $Q = 0.06$, and thus $X = 0.03$, or a 3% loss in sensitivity.

The EVLA will measure the system temperature following the sub-band filters, which can be set to 128, 64, 32, $\cdots$, 0.03125 MHz. If we presume that the cal signal is 5% of the cold-sky value, then eqn. (10) can be used to estimate the length of integration time needed to achieve the desired accuracy of 0.5%:

$$\tau = \frac{71}{B_{MHz}} \qquad \text{sec} \tag{13}$$

Thus, a 0.5% accurate visibility estimation can be made in 10 seconds or less for all sub-bandwidths of 8 MHz or greater. Given that the WIDAR correlator provides sub-bandwidths as narrow as 31.25 kHz (for which an integration time of nearly 40 minutes is needed to achieve the accuracy goal), the question of how to provide accurate gain calibration for narrow-bandwidth observations arises. This, and other issues relating to accurate measurement of system temperature, are discussed in the last section.

3 Results from the VLA's Tsys System

Does in fact the synchronous demodulation of the injected calibration noise provide a stable system temperature measurement with the predicted sensitivity, and its dependencies on bandwidth and system temperature indicated by the equations of the last section? To answer these questions, we have analyzed some data taken with the VLA.

The VLA records system temperature in two locations: A 'front-end' measurement, taken over a full 50 MHz bandwidth within the F4 module in the antenna, and a 'back-end' measurement in the T5 module, following the baseband filter selection. For both, the system temperature is derived from

$$T_{sys} = KT_{cal}\frac{V_{TP}}{V_{sync}} \tag{14}$$

where V_{TP} and V_{sync} are voltages provided by the electronics which are proportional to the total system power and the synchronous power, respectively. The factor K comes from the engineering design, and equals 15 for the FE measurement, and 10 for the BE measurement. For the FE measurement, T_{TP}

is fixed at 3.0 Volts, while for the BE measurement, it is at the value provided by the AGC circuitry, typically 5.5 Volts.

To test the derivations of the accuracy in system temperature measurements upon system temperature and bandwidth, we observed the strong source Cygnus A and a nearby calibrator at the standard C-band frequencies (4885 and 4835 MHz), with bandwidths of 50, 25, 12.5, 6.25, 3.12, 1.56, and 0.78 MHz. This band was selected as it is believed free of RFI – a critical issue in obtaining accurate system temperature values. The Tsys integration time is effectively about 1.0 seconds, due to internal time constants.

The values of system temperature derived are dependent upon the value of the noise diode calibration temperature – which is not in general acurately known[2]. The values for Tsys were corrected for this uncertainty by a scaling factor derived from the observed change in system temperature when observing Cygnus A. The antenna temperature due to Cygnus A (the increment in Tsys caused by the source flux density) should be

$$T_{CygA} = 2\epsilon/3 \tag{15}$$

where ϵ is the antenna efficiency in percent. Thus, for the measured efficiency of 60%, the system temperature should rise by 40K when observing Cygnus A. This value was used to calibrate the system temperature scale for each antenna and IF.

Ideally, the determination of system temperature for a continuum observation such as this would be independent of bandwidth. The only effect expected would be a decrease in the accuracy of the determination as the bandwidth narrows. But the observations show that there is a dependency of system temperature on bandwidth, as shown in Figure 1. The rise in system temperature is symptomatic for all EVLA antennas in this IF. If the rise were an effect due to system temperature only, then the increment due to Cygnus A should be constant at 40K – this is not the case, as the increment also rises with decreasing bandwidth. An increase in efficiency with decreasing bandwidth seems quite implausible, partly because the observed effect is reversed in IF 'C' – where the system temperatures decrease with decreasing bandwidth. We suggest that these apparent changes are caused by the synchronous system itself, and are not reflective of any change in system performance.

Equation (9) shows that the variance in derived system temperature depends on bandwidth and system temperature as

$$\sigma_T^2 = \left(\frac{2T_{sys}^2}{T_{cal}}\right)^2 \frac{1}{B\tau} \tag{16}$$

presuming that $T_{cal} \ll T_{sys}$. The rms error in the determination rises as the square of the system temperature because it depends both on the power of the signal, and on the ratio of the signal power to cal power. This relation can be expressed as

$$\log(\sigma_T^2) = 2\log K - \log B\tau \tag{17}$$

where $K = 2T_{sys}^2/T_{cal}$. Thus, a logarithmic plot of the variance against bandwidth should have a slope of -1, and an intercept dependent upon the system temperature and calibration diode temperature. Such a plot is shown in Fig 2 for two antennas. The slopes are indeed equal to that expected, within the errors, and indicate that there are no additional errors in the measurement system over the ~ 3 minute duration of the observation.

The difference in the intercept values between cold sky and Cygnus A provides an independent measurement of the system temperature. Assuming the increment in noise power by the calibration

[2] This uncertainty is not an important issue for VLA observation in general, as the error results in a scaling error in derived visibility amplitude which is the same for both source and the flux density calibrator. Observing a source of known flux density will correct the error. What is critical in this is that the fractional changes in system temperature be measured correctly.

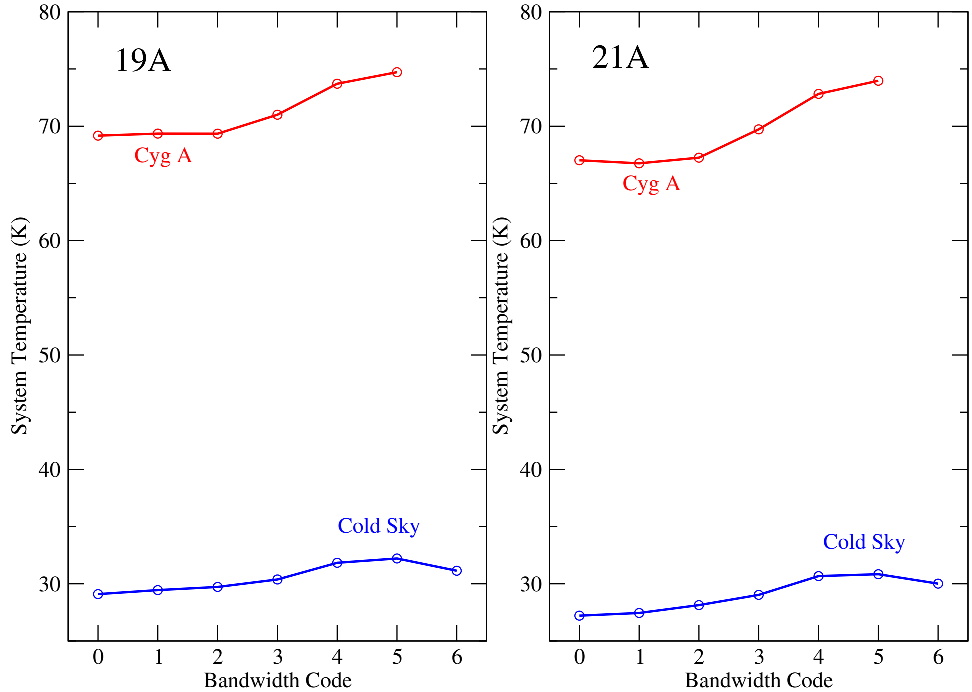

Figure 1: The derived system temperature for EVLA antennas 19 and 21, in IF ‘A’, as a function of bandwidth. The vertical scales for all bandwidths was corrected by the factor needed to make the increment equal to 40K at BW code = 0 (50 MHz).

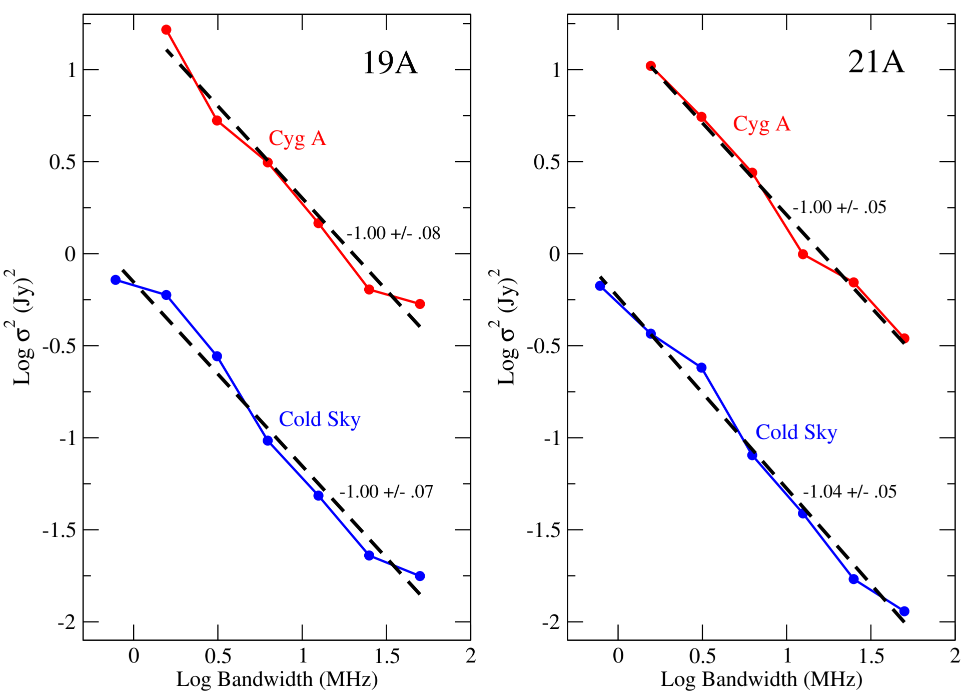

Figure 2: Plots of the variance in system temperature determination as a function of bandwidth, for two EVLA antennas in IF ‘A’.

signal is very small in comparison to the system temperature, the intercept difference is related to the ratio of the system temperatures as

$$\frac{T_{sys,hot}}{T_{sys,cold}} = 10^{\Delta/4}. \tag{18}$$

For both the antenna-IFs shown in the figure, the intercept separations are $Delta = 1.46$. Presuming the increment in system temperature due to Cygnus A is 40K, the system temperature is found to be 31K – very close to that derived through calibration of the system temperature via the antenna temperature of Cygnus A.

Finally, we look to see if the absolute values of the variance are as expected, given the known values of cold-sky system temperature, bandwidth, time averaging, and noise diode temperature. The observed variance at 50 MHz of about 0.015 Jy^2 is predicted with a system temperature of 30K and a calibration temperature of 4K.

In general, it is clear the system temperature measurement methodology is working well for the VLA.

4 Unresolved Issues Relevant to the EVLA

The preceding discussion presents the method and results for a working system in a benign enviroment – one generally free of interference with a relatively narrow fractional bandwidth. For the EVLA with the upcoming WIDAR correlator, we will be presented with a system which covers a much wider frequency span, and which provides a much wider range in bandwidth options.

The WIDAR correlator defines 128 sub-bands for cross-correlation, with 16 available for each of the eight input baseband signals. Each subband is independently tunable in width and center frequency. Two additional sub-band filters are available for each of the eight inputs – these can be independently moved to any frequency for monitoring purposes. Each sub-band's frequency response is shaped by up to four consecutive digital filters. The design allows the system power measurements for any sub-band to be made following one – and only one – of the cascaded filters. Hence, if a sub-band is being set up with a very narrow bandwidth, the total power measurements can be made on an upstream filter where the signal bandwidths are much wider.

The measurements are made by squaring and summing the input voltages on the fly. The fundamental time of measurement is 10 ms. A threshold voltage, above which data points are not utilized in the sum, is permitted, but there will be no opportunity to filter the data in any other way prior to the summation. Hence, statistical tests such as a median filter will not be supported. The correlator makes no assumption about the duty cycle of the calibration tone – changing the synchronous detection routine to scenarios where the calibration fraction is not 50% is straightforward, and can be modified by source name. The accumulated sums can be converted to system temperature values with any averaging time, independent of the cross-correlation integration time.

In addition to these correlator-related items, we will have two potentially useful monitoring points in the T304 downconverter modules. Each module will contain two power detectors the first at the input, the latter at the output. Both will produce samples at 500 Hz. A synchronous detector will be implemented for each in MIB software and the results made available as a monitor point. Each will produce the 'global-average' system temperature seen over the full bandwidth – up to 5 GHz wide for the input detector, and either 1 or 2 GHz wide for the output detector. These results are not intended for astronomical calibration, but should be useful for diagnostic information, such as time-variable power due to RFI, or monitoring system temperature behavior over the length of an observation.

We can identify a number of relevant issues regarding system temperature measurements with the new WIDAR system. These are listed below, in no particular order. Others can surely be defined with a little more thought. For some, the answers are fairly clear, for other, some more thought and testing will be required.

- Because of the wide frequency span of the correlator, it is virtually certain that at least a few of the 128 will lie atop spectral regions filled with detectable time-variable external interference. This is particularly true at the lower frequencies. How can we ensure a maximally stable and relevent measurement for those sub-bands which contain detectable RFI?
- A related issue is that of when we want the Tsys value to vary in response to time-variable emission, and when we do not. In general, it is clear that we do not want to react to narrowband external RFI, as those useful frequencies which are not contaminated by the interference see no change in system noise power. But what if the temporal variation is wideband in nature, such as emission from solar flares?
- The very narrow sub-bandwidth that WIDAR permits will be utilized for some specialized observations of narrow lines and (in particular) bi-static radar observations of planetary bodies. Obtaining high calibration accuracy within these sub-bands require impossibly long integration times. How are we to ensure accurate calibration? Given that the visibility accuracies are themselves much degraded due to the narrower channelwidths, is the 0.5% requirement relevant at all? We believe that a wider-bandwidth measurement, either picking off the values at an earlier stage in the cascaded filter chain, or by utilizing one of the two 'free' sub-band filters, will suffice. However, we must be careful not to utilize a wider bandwidth in situations where extra spectral noise power due to natural emission will be included – such as in L-band near the HI line. Although the line emission may be constant for the target source, it will not be present in the calibration observation at the same strength, so the added power will not be calibrated out correctly.
- For all WIDAR sub-bandwidths, over what length of time should we integrate the measurements before writing out a determined value? Should every output visibility be accompanied by a Tsys evaluation taken with the same integration time, or will a smoothed average be sufficient?
- The canonical $Q = 5\%$ calibration power is a nominal value, which varies over the band due to variations in both the cal spectral power and the frequency dependence of system temperature. Ideally, we would like to have the fractional cal power be a constant over the full band, but in practice the ratio is likely to vary widely over the band. Should we place requirements upon the engineers limiting the range of Q?
- For very strong sources, or in regions with bright background emission, the system temperature can be elevated by a factor of 10 or more. Attaining the same absolute gain accuracy would require a proportional increase in the cal power, or a much longer integration time. Is this necessary, and if so, how can we employ it? One possibility is to adjust the duty cycle of the cal-on power in response to the observed (or anticipated) system temperature of the observation.